Investigation of water spray evolution process of port water injection and its effect on engine performance

[1] School of Automotive and Transportation Engineering, Hefei University of Technology, Hefei, China

[*] Corresponding author: Yuan Zhuang, Email: zhuangyuan@hfut.edu.cn

Abstract

In this study, a 1.5L turbocharged gasoline direct injection (GDI) engine was modified by installing a port water injection (PWI) system adjacent to the intake valve to simulate the "quasi-direct" water injection. Experiments was performed at 1500rpm wide throttle open (WOT) condition to investigate the effect of PWI on knock suppression, and 4850rpm WOT condition to test the removal of fuel enrichment through PWI. Then, numerical simulation was conducted to investigate the water spray evolution process and subsequent influence on mixture formation. The experimental results showed that PWI could effectively suppress knock and decrease combustion temperature. Therefore, at 4850rpm WOT condition, the engine was able to operate at a stoichiometric air/fuel ratio with moderate advancement of spark timing. The combined effect finally resulted in nearly 6% thermal efficiency improvement. At 1500rpm WOT, 3.8% efficiency gain was achieved solely due to knock mitigation. Nitrogen oxides (NO_x), soot and hydrocarbon (HC) emissions also showed a decreasing trend with the increase of water injection amount. The simulation results indicated that about 80% of total injected water collided on the inner surface of the intake port which became the major source of water vapor. The portion of water vaporized in the air is small. Sufficirent time was important for intake port water film evaporation. PWI also resulted in in-cylinder wall wetting. The in-cylinder water wall wetting in 4850rpm was sober than that at 1500rpm due to stronger intake air motion and higher cylinder temperature. Although the general impact on the in-cylinder equivalent ratio is limited, it can lead to fuel-rich zone at the corner of the cylinder.

Keywords: Port water injection; Quasi-direct injection; Spray; Evaporation; Wall wetting

Abbreviations

ATDC	After top dead center	ISCO	Indicated specific carbon monoxide
BSFC	Brake specific fuel consumption	ISHC	Indicated specific hydrocarbon
BTDC	Before top dead center	ISNO	Indicated specific nitric oxide
CA	Crank angle	IVC	Inlet valve closure
CAN	Controller area network	IWI	Indirect water injection
CFD	Computational fluid dynamics	KLSA	Knock limited spark advance
CO	Carbon monoxide	NO	Nitric oxide
CO_2	Carbon dioxide	NO_x	Oxides of nitrogen
DDM	Diameter distribution method	ON	Octane number
DI	Direct injection	PDF	Probability distribution function
DWI	Direct water injection	PISO	Pressure-implicit with splitting of operators
ECFM	Extended coherent flame model	PWI	Port water injection
ECU	Engine control unit	RDE	Real driving emission
EGR	Exhaust gas recirculation	SI	Spark ignition
FSN	Filter smoke number	VVT	Variavle valve timing
GDI	Gasoline direct injection	WLTP	Worldwide harmonized light vehicles test procedure
HC	Hydrocarbon	WOT	Wide open throttle
IMEP	Indicated mean effective pressure		

1. Introduction

The fossil fuel depletion and the growing concerns on pollutant and CO_2 emissions lead the automotive industry to seek solutions through new engine technologies. Technologies such as high-boosting, direct injection, downsizing and hybridization are adopted to increase power density and reduce fuel consumption [1, 2]. In the turbocharged-downsized engines, the operation range of the engine will be shifted to a higher load condition where it is more prone to abnormal combustion, such as pre-ignition, knock and even super-

knock. The knock of spark ignition (SI) engines is a well-known abnormal combustion phenomenon that constrains engine performance and efficiency. It can result in a large pressure rise rate and great peak pressure, producing a larger sound and even severe damage to the engine. Implementation of water port injection had already shown the potential of mitigating the knock tendency and consequently thermal efficiency improvement ever since the study from the 1930s. Today, with the urgent needs of further development of downsizing technology and mandatory in real driving emissions (RDE) for engine stoichiometric operations at full load, water injection has regained interest and becoming imperative for SI engines.

The potential efficiency gains of water injection on engine performance are mainly through decreasing mixture temperature and the dilute effect of acting as an inert gas participating in the combustion process. Reducing mixture temperature is primarily induced by water droplets evaporation. Either by the form of indirect water injection (IWI, including port water injection (PWI) and plenum water injection) or direct water injection (DWI), it can effectively decrease the end gas temperature, which suppresses the knock tendency and enables the advance of combustion phase close to the optimum range. The engine thermal efficiency is increased consequently, and the compression ratio and charge pressure can be potentially enhanced. If the water is injected in the manifold or during the intake stroke by DWI, the lowed the mixture temperature increases the charge density, permitting higher volumetric efficiency as well as the engine power output. As the water enters the cylinder, it acts as an inert gas during the combustion process. The water vapor dilutes the mixture's oxygen concentration and brings down the real air/fuel ratio, resulting in elongated combustion duration and reduced maximum combustion temperature. The nitrogen oxides (NO_x) are therefore decreased. Furthermore, the dilute effect works with the reduced mixture temperature and raised heat capacity together to substantially lower down the exhaust temperature. This allows the avoidance of fuel enrichment during the full load condition, which improves the fuel economy and decreases the pollutant emissions such as hydrocarbon (HC) and carbon monoxide (CO). As for the negative side of elongated combustion duration, it can be easily compensated by advancing spark timing.

Recently, Thewes et al. [3] studied the trade-off between the rate of DWI and exhaust gas recirculation

61 in a single-cylinder gasoline direct injection (GDI) engine. The resulting fuel consumption benefit due to knock
62 mitigation in the WLTP cycle was 6.5% when compared to a modern concept engine that already equipped
63 with the variable compression ratio system. Lanzafame [4] examined using cheap low octane fuels in
64 combination with PWI to circumvent knock limits and conserve fuel cost. It was found that by implementing
65 compound injection mode, fuel with octane number (ON) as low as 66 could be reach the same engine
66 performance as high grade ON 95 gasoline. Younkins et al. [5] reported that the fuel consumption penalty
67 could be completely removed through PWI at full load, and an additional 35% NOx reduction was achieved
68 compared with no water injection condition. The CO and HC emissions also demonstrated 23.6% and 32.8%
69 reductions due to the stoichiometric air/fuel ratio thanks to the avoidance of fuel enrichment brought by water
70 injection. Gadallah et al. [6] compared the effect of different DWI strategies including injection at the suction,
71 compression and expansion strokes on engine emissions and efficiency improvement. It was reported that a
72 maximum reduction of 71% in NOx emissions was reached at a water injection rate of 14 mg/cycle and DWI
73 timing -60° CA after top dead center (ATDC). The indicated thermal efficiency improved the most by 4.2%
74 when water was injected during the compression stroke. While for water injection at suction and expansion
75 strokes, the efficiency improvements were 2.8% and 1.5%, respectively.

76 The water injection position is regarded as one of the key factors affecting the engine performance. DWI
77 can ultimately utilize water's great heat of vaporization to mitigate knock. A greater magnitude of the charge
78 cooling may be expected with DWI as all the water droplets evaporate in the cylinder. It also provides great
79 flexibility in controlling and optimizing as the water injection timing and quantity can be actively varied
80 according to the engine conditions. Compromising the volumetric efficiency is completely avoided in DWI
81 because the water liquid and vapor don't take up some volume of the fresh charge unlike what is happened in
82 PWI. Despite the merits, the high cost of the system and several engineering concerns such as dilution of
83 lubricant oil, the increase of complexity due to the additional injector, the durability of the high pressure water
84 pump and the cooling of water injector tip when it is not used are problematic issues hampering the real
85 implementation of DWI technology. For PWI configuration, water droplets can be well evaporated and mixed

with the fresh charge owing to the relatively long time between the end of water injection and combustion. The water droplets evaporate during the intake followed by increased volumetric efficiency and a decreased combustion temperature. It also shows potentially less in-cylinder wall impingement and thus reduced oil dilution issues. Recent studies also show that an installation of water injector close to the inlet valve is almost a "quasi-direct" water injection that achieves similar effectiveness of DWI while reducing the wall film formation which lowers the effectiveness of the water injection. In combination with the low cost of PWI system and easy to place injector along the intake port line, PWI configuration is considered as a practical solution for implementing water injection technology on SI engines.

Up to now, the published literature on the application of "quasi-direct" PWI was limited. Pauer et al. [7] investigated the position of the injector in the intake duct and they found that a position closer to the intake valves reduced the water consumption to less than 50% compared to an upstream position. Battistoni et al. [8] numerically evaluated several water injection strategies including PWI, DWI and manifold water injection. It was found that the location and targeting of the water injector were important, and PWI with injector close to the inlet valves allowed substantial gains in terms of combustion control and knock suppression. Vacca et al. [9] analyzed the thermodynamic effects of DWI and PWI through a 3D-CFD-tool QuickSim and pointed out that by optimizing the water injection strategies, PWI could realize the same gas temperature reduction as DWI or even better. DeBellis et al. [10] tested "quasi-direct" PWI strategies on a single-cylinder research engine. They found that a reduction of brake specific fuel consumption (BSFC) of up to 15-20% was possible for "quasi-direct" PWI while the maximum realized BSFC was 13.7% for manifold water injection. Generally, the number of experimental investigations for "quasi-direct" PWI was few. More tests on different engine types should be conducted to provide a more general conclusion of this kind of water injection configuration.

Another problem for "quasi-direct" PWI is that despite PWI ensures a long time for water vaporizing process, the different properties of water respect to gasoline also make the water evaporation process more complex. The water saturation pressure is 15 times less than gasoline, its surface tension and density are almost 3 times and 1.3 times of gasoline. These properties make the water not only shows worse volatility but also a

lower breakup tendency and higher probability in liquid film formation compared with gasoline. A largely different amount of vaporized mass between the two is expected if they are injected under the same condition. Thus, the water evaporation process is crucial because all the benefits of water injection are available only if it is vaporized. However, this process in real engine scenarios can only be well solved by numerical simulation and this kind of investigation is seldom reported in previous studies. Furthermore, most of the previous studies on the "quasi-direct" PWI strategy reported the experimental and numerical works separately. The micro and macro experimental results of PWI cannot be well correlated in this way, which may hamper the comprehensive understanding of this technology and further optimization on a real engine.

This study aims to solve these issues by comparing and analyzing both experimental and numerical outcomes to explore the potential of a "quasi-direct" PWI strategy. The investigation was first conducted on a state-of-the-art 135 kW 1.5L turbocharged GDI engine featured with a compression ratio of 11.7 and miller cycle. Then, the numerical simulation was performed with a special focus on the water evaporation process and its subsequent influence on mixture formation. The CFD simulation results were used to assist better understanding and explanation of the corresponding experimental results.

2. Engine and instrumentation

The experiments were conducted on a production 1.5L turbocharged GDI engine with a compression ratio of 11.7 and incorporated with miller cycle. The maximum power of the engine is 135kw at speed of 4850rpm and the maximum speed is 5500rpm. The specifications of the engine can be found in Table 1. The schematic of the engine test rig is shown in Fig. 1.

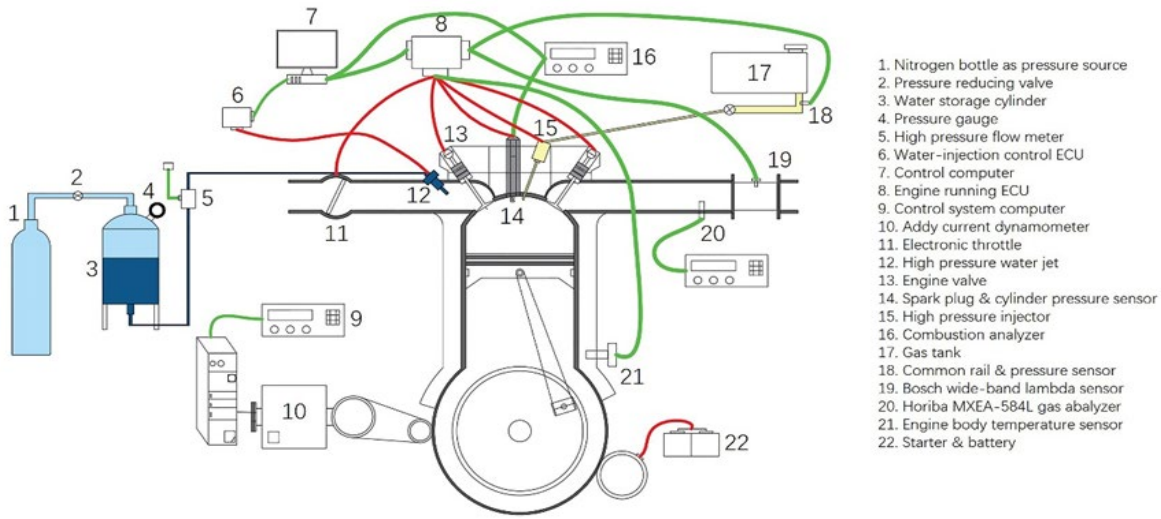

Fig. 1. Schematic of the test rig.

Table 1

Specifications of the test engine

Engine type	L4, four-stroke, water cooling
Compression ratio	11.5
Bore x stroke	75mm x 84.8mm
Engine capacity	1.5L
Intake and exhaust control	VVT
VVT adjustment range	0-60 ° CA
Intake Valve Open	341.5 ° CA @1500rpm; 352.5 CAD@4850rpm;
Intake Valve Close	596.5° CA @1500rpm; 628.5 CAD@4850rpm;
Exhaust Valve Open	149 ° CA @1500rpm; 125 CAD@4850rpm;
Exhaust Valve Close	336 ° CA @1500rpm; 356 CAD@4850rpm;
Fuel supply	Direct injection
Water supply	Port injection

The engine power is absorbed by a CW160 eddy current dynamometer produced by Kaimai (Luoyang) Electromechanical Co. Ltd. The corresponding engine bench numerical control device model is FST2D. The original ECU was replaced with an open access version control via “INCA” software, which provided the flexibility of adjusting the engine parameters to adapt to the implementation of water injection. Thus, at full load condition, the fuel enrichment was originally used to limit the turbine inlet temperature according to the engine MAP, but can be manually removed due to the additional cooling provided by water injection. The cylinder pressure was averaged from 200 consecutive cycles and acquired via a Kistler 6115B pressure

transducer incorporated in the spark plug with a sample rate of 720 times per cycle. The collected signal was processed and monitored by an AVL Model 642 combustion analyzer which also was used for the analysis of the combustion characteristics and the determination of the engine knock limit. The knock limited spark advance (KLSA) in this test was set as the peak to peak cylinder pressure oscillation over 1.0 Bar when 10 out of 100 consecutive cycles were detected such abnormal, as suggested by the engineer from engine manufacturer. The Horiba Mexa-7500 was implemented in the 1.0 meter from the exhaust valve in order to measure emissions of HC, CO and NOx.

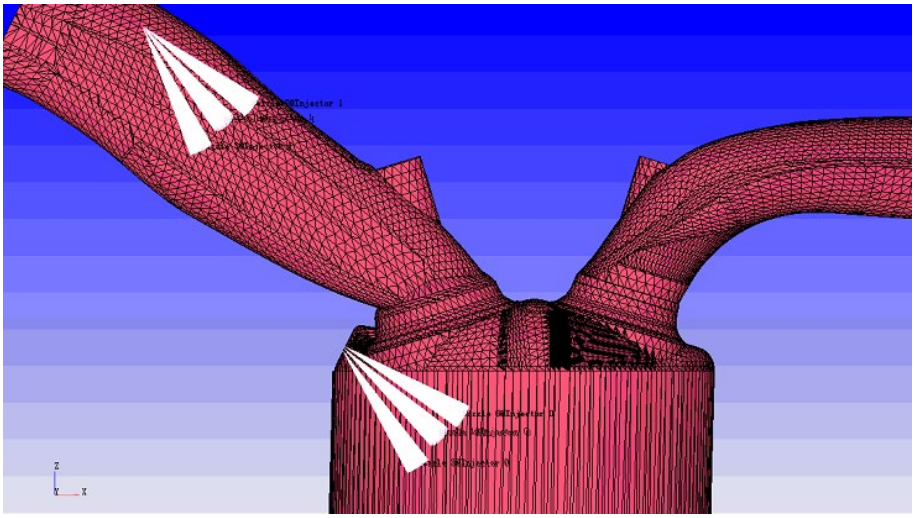

(a)

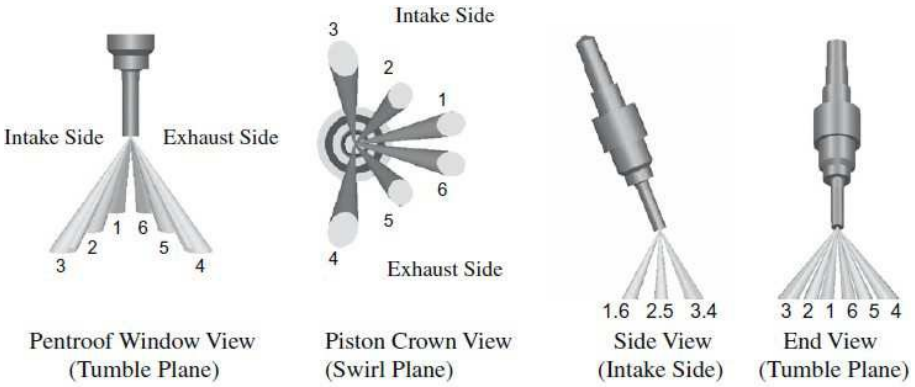

(b) (c)

Fig. 2. Injector locations and spray patterns

(a) Computation grid and relative positions of PWI and GDI; (b) Nominal spray pattern of the injector used: engine views; (c) Nominal spray pattern of the injector used: pressure chamber views.

The gasoline fuel injector is lateral mounted under the intake valve. It is a six-hole injector with a spray

cone angle of 34° and a 17° bent axis (Fig. 2). The gasoline fuel injection pressure was kept at 15 MPa. The air/fuel ratio was kept at stoichiometric value even at full load condition. The PWI injector used in the test was the same as that use for the gasoline fuel. It was placed about 10 cm upstream of the inlet valve with a 30° bent angle between the intake port horizontal plane (Fig. 2). This adjustment is to let each half of its spray plumes targeting the corresponding inlet valve (each cylinder has two intake valves). Such installation was expected to create a dense cloud of small water droplets in the vicinity of the inlet valve. Once the inlet valve was open, water penetrated in the cylinder and rapidly evaporated, generating the expected cooling effect, so that the "quasi-direct" water injection could be realized. The water injection pressure during the test was set at 5 MPa via a 35 L water tank pressurized by nitrogen. The PWI injectors were activated by an independent ECU which was connected with engine onboard ECU through CAN bus to synchronize the crankshaft and camshaft signals. An additional" INCA" software was used for the controlling of water injection timing and quantity. The relation between injector pulse wide and water injection quantity was statically calibrated before the experiment to ensure accurate control of the water injection. During this test, each experimental condition was repeated at least three times to increase reliability. The measurement uncertainties were determined using the method given in Ref. [11] . The uncertainties of the testing devices are shown in Table 2. More details of the engine test rig can refer to [12] .

Table 2

Measurement uncertainties.

Device	Associated measurement uncertainty
Engine speed	0.25% of full scale
Torque	0.03 of the output voltage
Air volumetric flow rate	4.0% of the measurement
Gasoline mass flow rate	1.8% of the measurement
Water mass flow rate	1.9% of the measurement
In-cylinder pressure	0.45% of full scale
HC concentration	3.1% of the measurement
NO concentration	3.5% of the measurement
CO concentration	3.1% of the measurement

Filter smoke number	2.8% of the measurement
Bosch lambda sensor	1.6% of the measurement

3. Selection of test conditions

The engine was first warmed up and raised to the designated speed. Then, the throttle valve was gradually opened to wide-open throttle (WOT) after the circulating water temperature was around 90 ± 3 °C. Two engine speeds of 1500rpm and 4850rpm were selected for this test as the 1500 rpm WOT is the condition where the propensity of knock was large, and 4850rpm WOT was the engine maximum power condition where fuel enrichment was normally adopted to limit the exhaust temperature for the protection of turbine. Thus, in this way, the most beneficial effect of water injection on knock mitigation and stoichiometric combustion at full load condition can be evaluated. Once the engine was stable at designated speed, the water injection was initiated with the three fixed quantities of 10.34 mg, 17.1 mg and 25.2 mg. The spark timing was then advanced accordingly until KLSA was reached. At 4850 rpm, the air/fuel ratio was first leaned to guarantee stoichiometric combustion then the spark timing was varied if there is still room for this optimization. When the knock was detected via monitoring AVL indicom, the spark timing was then retarded 1° CA and marked as adjusted KLSA. The reason for keeping water injection pressure at 5 MPa was because the surface tension of water (72 mN/m) is much larger than that of gasoline (22 mN/m). Therefore, to achieve a better atomization and provide enough momentum for water droplets directly entering cylinder, higher PWI pressure greater than convention 0.5 Mpa or 1.0 Mpa was selected for this investigation and this pressure was also used by Hoppe et al. [13]. The PWI injection timing was fixed at 320° CA BTDC in order to ensure all the water injection taking place while the inlet valve was open. The engine test conditions and the corresponding nomination are shown in Table 3.

Table 3

Test conditions.

speed/rpm	Fuel injection/mg	Water injection/mg	W/F	Nomination
1500	51.6	0	0%	L0

		10.34	20.0%	L10
		17.1	33.1%	L17
		25.2	48.8%	L25
4850	58.26	0	0%	H0
		10.34	17.7%	H10
		17.1	29.3%	H17
		25.2	43.3%	H25

4. CFD engine model

Three-dimensional CFD software AVL Fire was used in this study to investigate the effects of PWI on water evaporation, mixture formation and combustion processes. To save computation time, the exhaust and intake port grids were was deleted after the exhaust and intakes valves were closed, respectively. The basic size of the grid was 1.5 mm and the mesh was refined at the valves and spark plug regions to improve the mesh quality. The mesh dependency study was performed at the top dead center. The in-cylinder pressure traces with different meshes of 2.842×10^5, 3.154×10^5 and 3.720×10^5 have been compared. Strong grid dependencies were not observed during the simulation. Therefore, the Mesh with 2.842×10^5 nodes was finally selected for this investigation.

A brief description of models used in the numerical simulation is in the following. The Realizable k-ε turbulence model was used to calculate in-cylinder turbulent flow. The traditional standard k-ε model cannot provide enough accuracy in the prediction of the spreading rate of both planar and round jets especially in dual-fuel injection conditions. Therefore the Realizable k-ε turbulence model was selected. The Walljet model was chosen for fuel-wall interaction simulation.

The calculation of conservation equations of mass, energy and momentum and heat transfer equation between the wall and airflow were solved in each 0.25° CA time step. During the periods of inlet or exhaust valve opening and closing, gasoline and water injection, the time step was reduced to 0.1° CA to prevent divergent calculation. The PISO (Pressure-Implicit with Splitting of Operators) was introduced in the pressure-velocity coupling scheme to optimize the computational efficiency for compressible flows. The spray models

were based on a statistical method referred to as dicrete droplet model (DDM) [14]. A set of sub-models were adopted to take into account of the effects of break-up, fuel evaporation, droplet-gas momentum exchange, droplet-wall interaction. The enable model was selected for turbulent diffusion simulation of gasoline and water droplets and the multi-component model was used for their droplets evaporation. The primary breakup process (blob injection concept) was modeled by Rosin-Rammler Diameter Distribution Method which was based on the assumption that an exponential relationship existed between the droplet diameter (d) and the mass fraction of droplets with the diameter greater than d. The secondary droplets breakup process was simulated by the WAVE model which was regarded as appropriate for high Weber number (We >100) flows because it considered the breakup of the droplets caused by the relative velocity between the gas and liquid phases [15, 16] . The O'Rourke and Amsden model was chosen in this study for the wall-film model which was used to calculate the collision of liquid with the wall driven by the initial momentum of fuel injection or airflow. The diameter, velocity and mass ratio of the rebound or splash droplet were modeled by the droplet collision model. The combustion process was modeled using the Extended Coherent Flame Model (ECFM) -3Z model with the partially premixed combustion concept in which both the mixture fraction and progress variable were solved [16-18] . The combustion process was initiated by releasing a specific amount of energy to the cells at the spark plug gap at the spark timing. The presumed PDF look-up table was used to model the turbulence–chemistry interactions. The chemistry look-up tables were generated using complex reaction mechanisms which incorporated the latest insights on combustion chemical kinetics [19] . A three-dimensional PDF table was generated to determine the temperature, density, and species fraction in the turbulent flame. Finally, the thermal NO formation was modeled by the extended Zeldovich mechanism.

The boundary and initial conditions were set up based on the experimental conditions. The typical wall temperature distribution for turbocharged SI engines at normal steady-state conditions was used for this study. The temperature of 600 K, 458 K, 573 K, 523 K and 923 K were employed for cylinder head, cylinder wall linear, the piston up-surface, intake valve and exhaust valve, respectively. The intake and exhaust ports wall temperatures were set at 333 K and 783 K respectively. The inlet and outlet pressure values were set according

to the pressure sensor installed on the intake and exhaust ports, which were 1.6 and 1.8 bar, respectively. The room temperature of 298 K in the engine test rig lab was used for intake air temperature. Other initial conditions were set up according to the measured in-cylinder pressure and exhaust gas temperature.

The spray models used in the simulation were first verified by comparing the simulated and measured spray structures`. The water spray was experimentally calibrated in a constant volume chamber providing boundary and initial conditions similar to water spray modeling. The orifice diameter of the Bosch six-holes injector used for this test is 0.15 mm. A 50×10 mm (radius×length) cylindrical domain was created to perform the validation modelling. Fig. 3 compares the experimental and simulated results of the water and gasoline spray patterns after 2ms of injection at the injection pressure of 5 and 15 MPa, respectively with ambient pressure of 0.1 MPa. It can be seen that the spray shape and the penetration length of experimental results are in good agreement with the simulated ones, indicating that the spray model can well represent the spray characteristics of the water spray for the engine simulation.

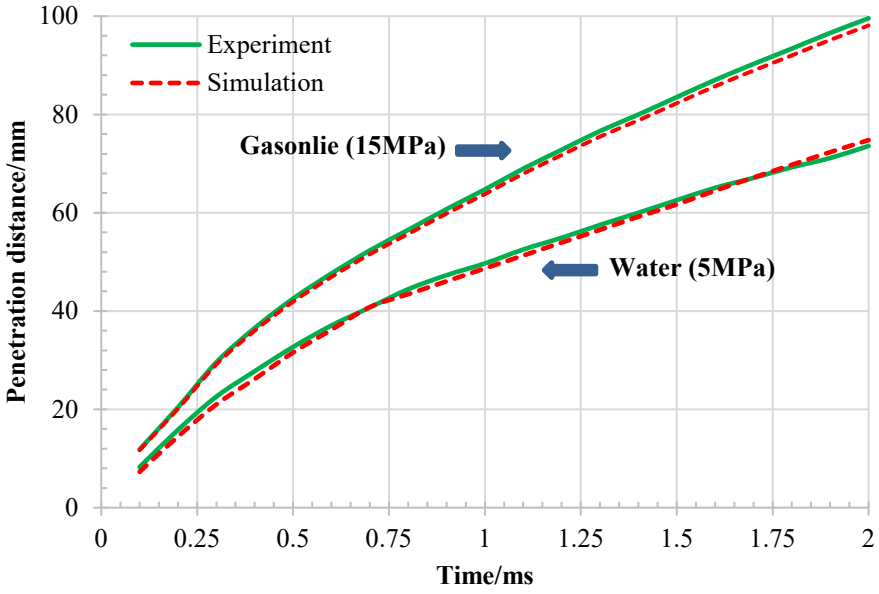

(a)

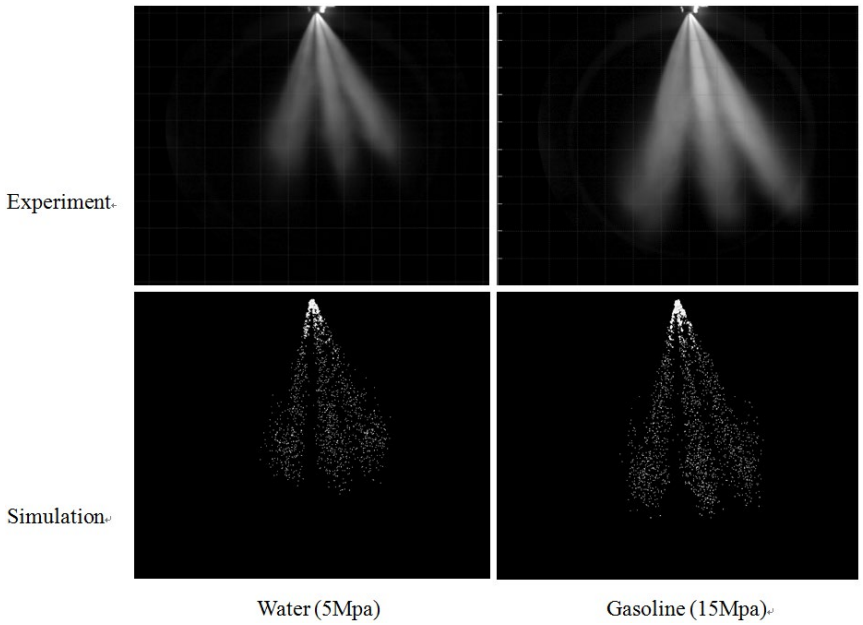

(b)

Fig. 3. Comparison of the spray experimental and numerical results
(a) Penetration distance; (b) Spray pattern

Then, the spray model was incorporated into the engine model for the simulation of mixture formation and combustion processes. It simulated the process starting from PWI injection (320° CA BTDC) and ending at the exhaust valve opening (336° CA ATDC). Fig. 4 shows the comparison between the numerical and experimental results of the in-cylinder pressure and heat release rate, including both pure gasoline (Fig. 4a) and PWI (Fig. 4b) conditions. The water injection amount was 25 mg and spark timing was KLSA. It can be seen that the experimental and numerical outcomes agree well. Thus, the engine model can well reflect the working process of the engine, and the engine water spray can be deeply studied in the form of numerical simulation.

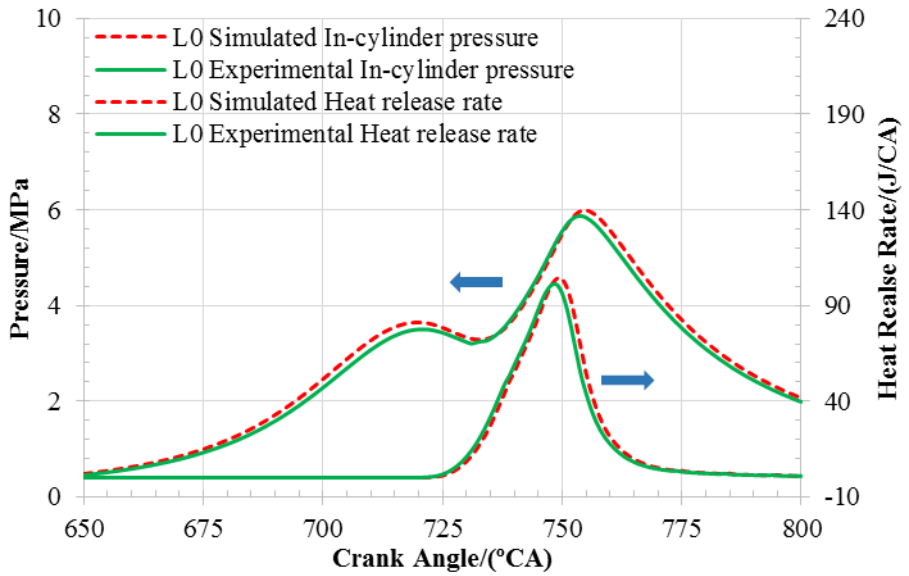

(a)

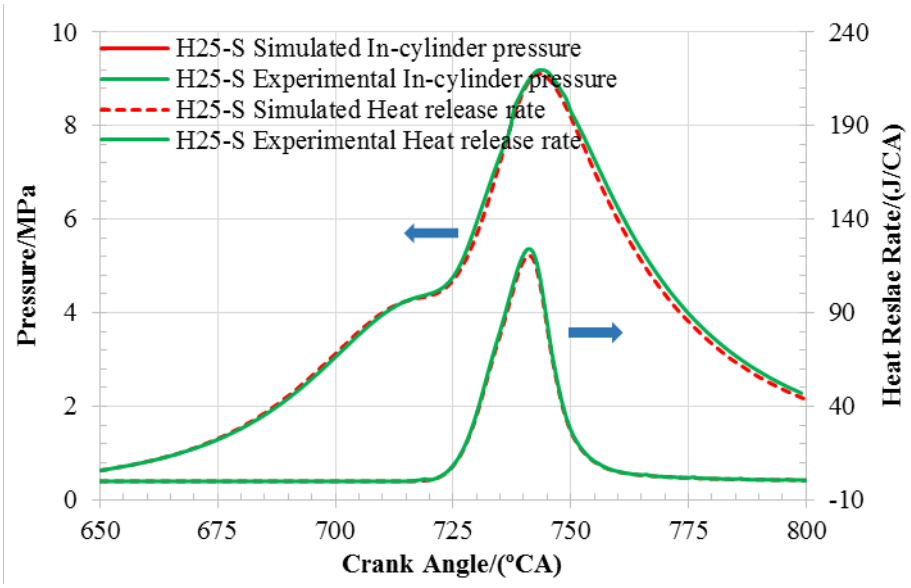

(b)

Fig. 4. Comparison between experimental and simulation results on In-cylinder pressure and heat release rate (a)L0 Pressure and heat release; (b)H25-S Pressure and heat release

5. Results and analysis

In this section, the test results of "quasi-direct" PWI are first presented, including engine performance, combustion and emissions at two representative conditions of 1500rpm WOT and 4850rpm WOT. Then, the numerical simulation with the special focus on water evaporation process and corresponding influence on mixture formation is discussed.

5.1 Effect of PWI on engine performance and emissions

Fig. 5 illustrates the variations of IMEP and spark timing advancement with the water injection amount. Error bars are added for the IMEP, representing the uncertainty range. As can be seen in the figure, the IMEP increases monotonously with the raise of water injection amount in both tested speeds. At 1500rpm, the IMEP increases from 18.2 bar to 22.7 bar when water injection amount is raised from 0 to 25 mg, while at 4850rpm, the IMEP augment is 3.7 bar, from 21.4 bar to 25.4 bar. The raise of IMEP is mainly attributed to the advance of spark timing thanks to the mitigation of knock by water injection. It should be noted that at 4850rpm when the water injection amount is 10mg, the spark timing increment is little, only 0.5° CA. This is because 4850rpm WOT is the maximum power condition, where the fuel enrichment is applied to keep the exhaust temperature within the safety range of 875° C for the protection of the turbocharger. At the water injection amount of 10mg, most of the heat absorbed by water evaporation is used for comprising fuel enrichment by substituting the cooling provided by extra gasoline, but not for reducing the in-cylinder temperature to suppress knock. The dilute effect of water vapor also provides additional benefit on knock suppression through reducing mixture energy density [20]. This may explain why the spark timing can still have little advancement when the water injection amount is only 10mg, where the lambda (λ) is 0.96 which means the amount of injected water is unable to provide enough cooling to completely waiver fuel enrichment or knock suppression. As the water injection amount raises to 17mg, the cooling provided by water is not only enough to completely remove fuel enrichment but also gives additional cooling for knock mitigation, permitting 2.2° CA spark timing advancement when compared with no water injection condition. Therefore, at 4850rpm the IMEP increment is marginally with water injection of 0-10mg, and becomes large with 17-25mg.

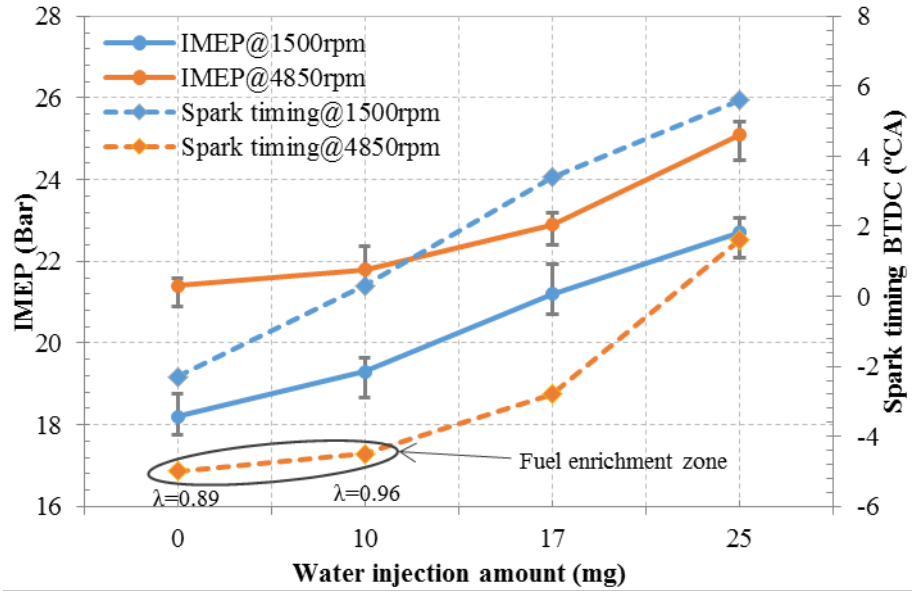

Fig. 5. Variations of IMEP and adjustment of spark timing with water injection amount.

Two of the engine operating parameters that PWI influences most are the intake and exhaust temperatures. Fig. 6 gives the variations of intake and exhaust temperatures with the water injection amount. It should be noted that the intake temperature is measured through the thermal couples installed at end of each intake ports just 4.5cm before the inlet valve, which give more accurate information of charge temperature variation caused by "quasi-direct" PWI. As shown in Fig. 6, the intake temperatures at both 1500rpm and 4850rpm first decrease with the rise of water injection amount, and reach a bottom of 38° C at water injection amount of 10mg for 1500rpm and 42° C at water injection amount of 17mg for 4850rpm, respectively. After that, the intake temperature shows a slight increase with the further aggrandizing of the water injection amount. The stall of further reduction of intake temperature is mainly due to the water wall wetting. When water injection amount is greater than 10mg at 1500rpm and 17mg at 4850rpm, water impingement on intake port becomes severe and the evaporation of such water does not absorb heat from the air but from the intake port and valve seat. Detailed analysis of water impingement and evaporation process will be elaborated in section 3.2.

The exhaust temperatures at both tested conditions show a continual downtrend with adding of water injection amount. At 4850rpm, it reduces from 921° C which is approaching the temperature limit for the compressor of 950° C, to 867° C when the water injection amount raises from 0 to 25mg. For 1500rpm, about

48° C exhaust temperature drop is realized by water injection, from 732° C down to 684° C. The decrease of exhaust temperature is primarily caused by the cooling and dilute effects of PWI [9, 21]. For the cooling effect, the evaporation of water droplets decreases the fresh charge temperature as well as the initial combustion temperature. Similar to EGR, the dilute effect reduces the mixture energy density, combustion velocity and combustion temperature. Therefore, the exhaust temperature lowers down with the increase of water injection amount. It is worth noting that the spark timing advances as the water injection amount raises, which makes the combustion happens in smaller cylinder volume, resulting in high combustion pressure and temperature. Theoretically, the exhaust temperature should increase with the advance of spark timing. However, in this test, the result is opposite to that. This indicates that water injection has greater potential in reducing exhaust temperature. Thus, further enhancing thermal efficiency by optimizing spark timing and higher boost ratio can be realized at stoichiometric air/fuel ratio at full load condition through the introduction of water injection.

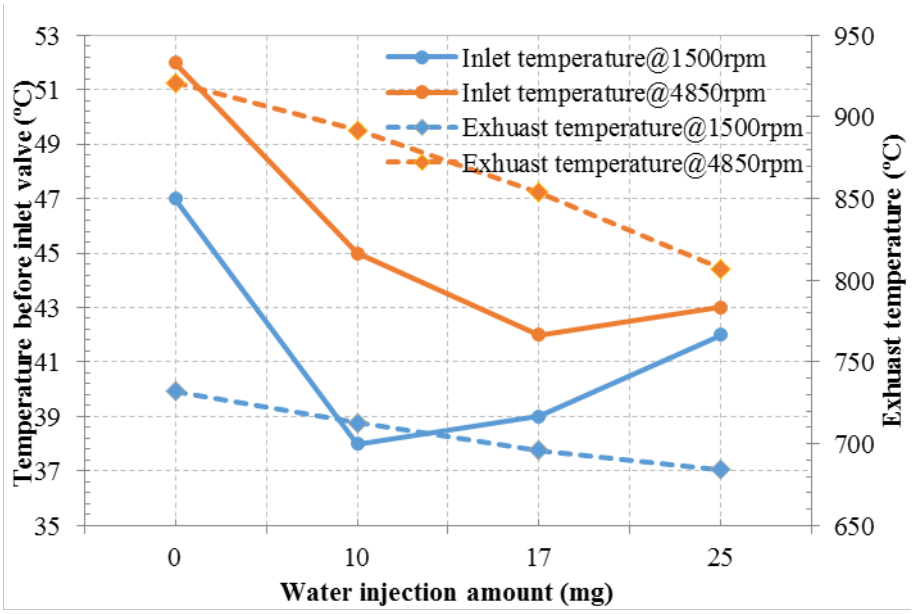

Fig. 6. Variations of temperature before inlet valve and exhaust temperature with water injection amount.

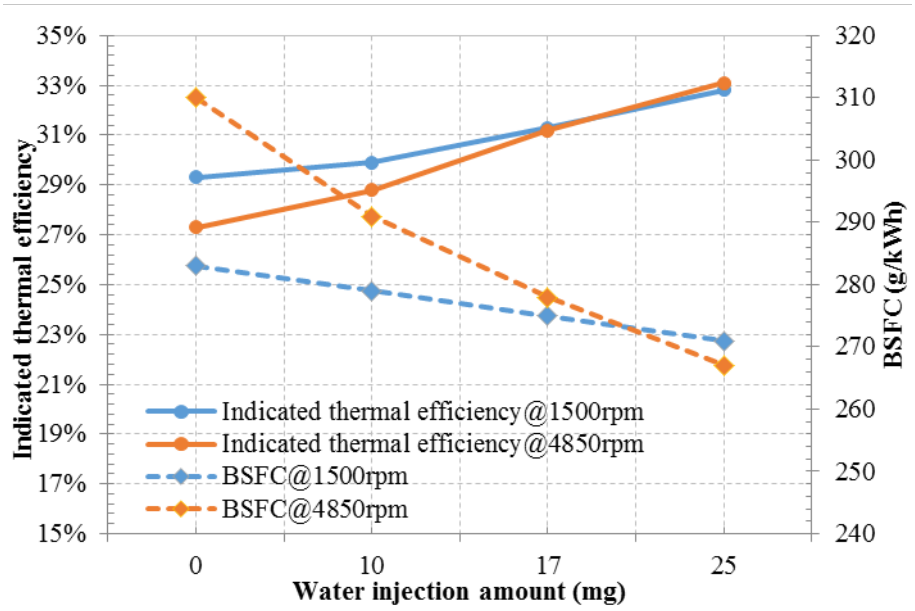

339

340 **Fig. 7.** Variations of indicated thermal efficiency and BSFC

341 The variations of indicated thermal efficiency and BSFC with water injection amount are shown in Fig.
342 7. As it can be seen in the Figure, the indicated thermal efficiency and BSFC at 4850rpm demonstrate the
343 largest variation. At 4850rpm, the indicated thermal efficiency raises from 27% to 33% and the BSFC falls
344 from 310 to 267 g/kWh when the water injection amount is increased from 0 to 25mg. This should be mainly
345 attributed to the removal of fuel enrichment. The fuel enrichment uses additional gasoline to cool down the
346 exhaust temperature for the protection of turbine, irrespective of its compromise on efficiency, fuel
347 consumption as well as emissions. At 4850rpm, a more optimum combustion phase also contributes to the
348 improvement of indicated thermal efficiency and BSFC when the water injection amount is greater than 17mg,
349 above which the cooling brought by water is not only sufficient for canceling fuel enrichment but also well
350 enough for permitting more spark timing advancement. For 1500rpm, the injected water is only used for
351 suppressing knock allowing more advanced spark timing. The indicated thermal efficiency improvement and
352 fuel conservation are not comparable to those at 4850rpm. Despite that, the improvements at 1500rpm are also
353 considerable, as the indicated thermal efficiency is increased by 3.8% and BSFC is reduced by 22 g/kWh.
354 Generally, the fuel enrichment is greatly adverse to thermal efficiency and fuel economy, and water injection
355 has the potential to overcome this shortcoming.

356

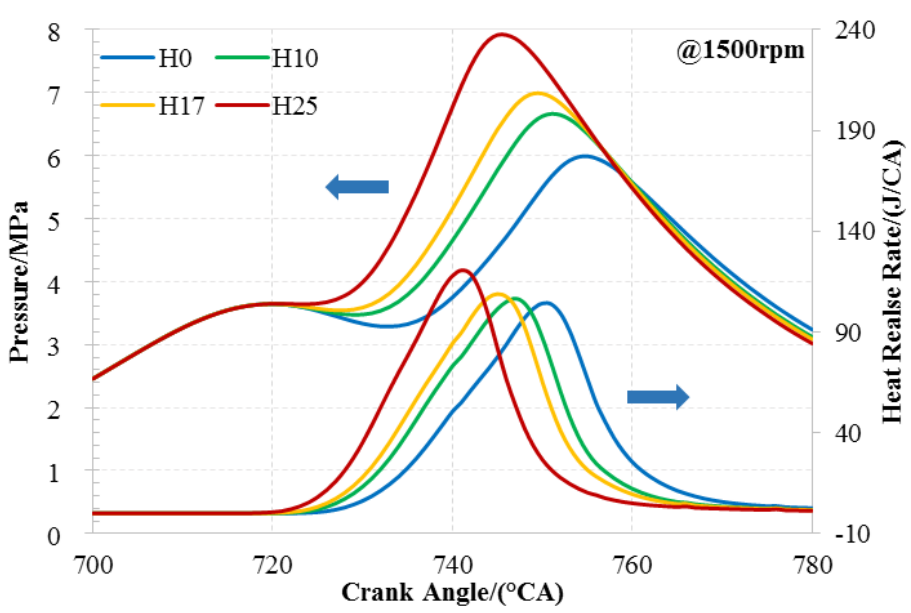

(a)

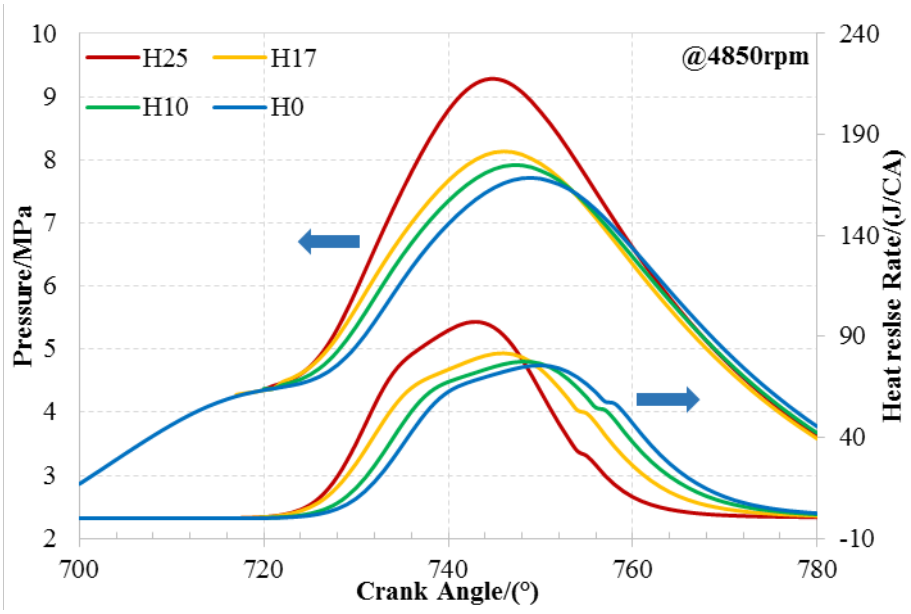

(b)

Fig. 8. In-cylinder pressure and heat release rate
(a) @1500rpm WOT; (b) @4850rpm WOT

Fig. 8 shows the pressure traces and corresponding heat release rate curves for water injection amounts of 0mg, 10mg, 17mg and 25mg at 1500rpm and 4850rpm, respectively. It clearly shows that the raised water mass results in higher and earlier peak in-cylinder pressures. This is especially obvious at 1500rpm and 4850rpm when the water injection amount ascends from 17mg to 25mg. The higher and earlier peak in-cylinder pressure resulted from advanced spark timing allows more combustion to take place in small cylinder volume,

thus releasing heat more intensively. Correspondingly, the peak in-cylinder pressure increases, and the heat release duration reduces. For 1500rpm, the injected water primarily contributes to the knock mitigation. Therefore, the spark timing advancement is substantial for each increment of water injection amount (Fig. 5). However, for 4850rpm, the injected water is first used to ameliorate the thermal load of the turbine and thus providing less cooling to suppress knock. Consequently, the spark timing increment is marginal with 0~10mg water injection. This phenomenon is improved after the water mass reaches 17mg, and the spark timing increases 4.4° CA when the water injection amount is increased from 17mg to 25mg. Therefore, the big leap of in-cylinder pressure can be seen at 4850rpm and the water injection amount of 25mg.

For better analysis, the effect of water injection on the combustion phases of CA50 and CA10-90 is shown in Fig. 9. CA50 refers to crank angle where 50% accumulated heat is released, and major combustion duration (CA10-90) is defined as the crank angle degrees from 10% to 90% of fuel mass burnt. In line with the results shown in Fig. 8, Fig. 9 shows that CA50 advances from 36.1 to 26.1° CA BTDC at 1500rpm and from 30.1 to 24.5° CA BTDC at 4850rpm with water injection. It is generally regarded that keeping CA50 between 8 and 10° CA ATDC can reach optimum engine efficiency. The advanced combustion phase should be one of the main factors that contribute to the increase in indicated thermal efficiency. Fig. 9 also shows that CA10-90 at both tested speeds decrease with the raised water injection amount due to the spark timing advances. However, water injection can dilute the mixture energy density, reduce the actual air/fuel ratio, and decrease radicals of O, OH and H due to the great three-body effect of water. These factors should theoretically result in lower flame speed and elongated combustion period. The reduced CA10-90 indicated that the negative effect of water injection on combustion speed can be compensated by the advance of spark timing.

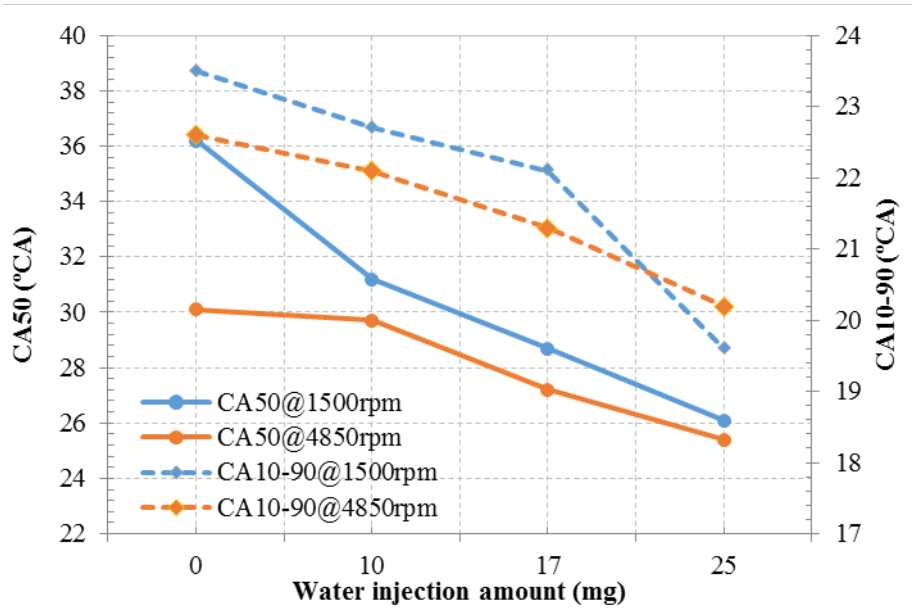

Fig. 9. Variations of combustion phasing (CA50) and major combustion duration (CA10-90).

Fig. 10 shows the variations of ISHC and ISCO. At 4850rpm, the ISCO and ISHC first decrease with the increase of water injection amount until 17mg, then the downward trends slow down with an even slightly increase of HC emissions when the water injection mass raises to 25mg. For 1500rpm, the ISHC gradually aggrandizes with the raise of injected water mass and ISCO shows an opposite trend to that of ISHC. The substantial decreases of ISHC and ISCO at 4850rpm with 0-17mg water injection are because of the revive of stoichiometric combustion. The λ is between 0.89-0.96 at 4850rpm with 0-10mg water injection (Fig. 5). The rich mixture combustion normally yields high HC and CO emissions due to incomplete oxidization. As λ decreases to stoichiometric value, the HC and CO emissions decrease consequently. The slight increase of ISHC at 25mg water injection can be attributed to the raised in-cylinder pressure (Fig. 8(b)) which traps more unburnt products in crevice volume during the combustion, and the existence of water which brings down the combustion temperature and dilutes the oxygen density. The decreasing trend of ISCO at 1500rpm may be because of the increase in the OH radical concentration when water participates in the combustion process [22, 23], which is conducive to the oxidation of CO.

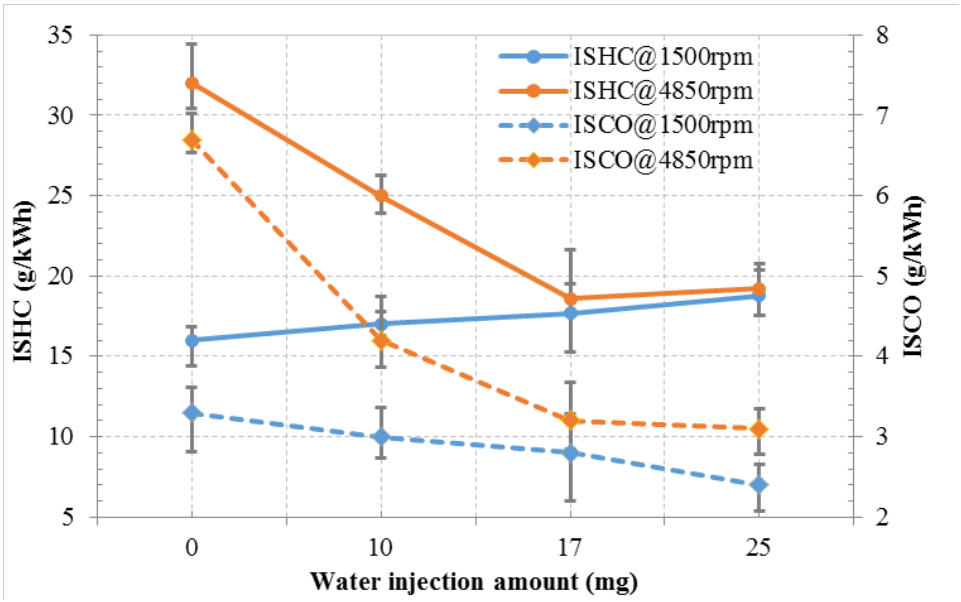

405

406 **Fig. 10.** Variations of ISHC and ISCO

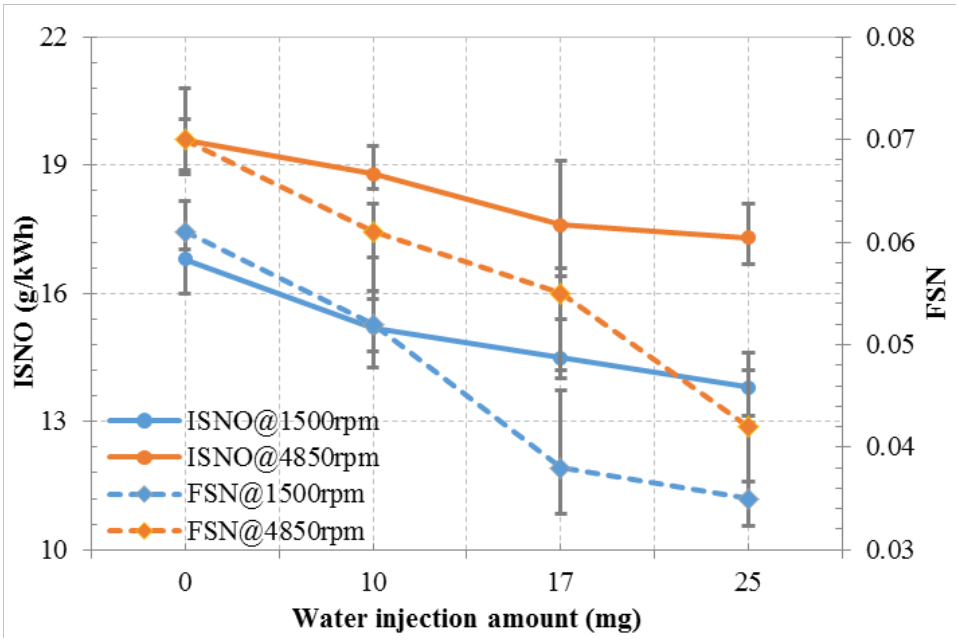

407

408 **Fig. 11.** Variations of ISNO and major FSN

409

410 Fig. 11 illustrates the trends of ISNO and filter smoke number (FSN) at different water injection amounts.

411 Apparently, both ISNO and FSN show a linear decrease trend with the increase of water injection amount. It

412 is widely accepted that water reduces NOx emissions via thermal and chemical effects. For the thermal effect,

413 water injection reduces the in-cylinder temperature due to cooling and dilution effects. Chemically, water vapor

414 can further reduce the O radical concentration by the scavenging reaction ($H_2O + O = 2OH$), which reduces

415 NO_x. For FSN, lower burning temperatures due to the use of water injection should be the main reason for the

soot emission reductions. Under high temperature, water is dissociated into H and OH radicals. It has been proven that OH radicals are remarkably effective in oxidizing soot precursor species [24-26].

5.2 Evaluation of intake port water evolution process

Numerical simulation is performed in this section to investigate the water evaporation and wall-wetting characteristics. As the final benefits of water injection are all depending on the status of injected water, the water spray evolution process is crucial and directly affects the combustion and emission formation processes. Fig. 12 illustrates the intake port water film distribution at 1500rpm and 4850rpm with the water injection amount of 10mg, 17mg and 25mg, respectively. The left column shows water film distribution when 50% of water is injected, the middle column demonstrates the graphic with the maximum water film thickness, and the right column is the wall-wetting characteristic after 20° CA of the inlet valve closed. Generally, in both 1500rpm and 4850rpm conditions, the wall-wetting becomes severe with the increase of water injection amount and the wall-wetting area and thickness do not see significant shrink until the inlet valves are closed. The water film mainly concentrates on the bottom side of the inlet port. It stretches from the downside of the injector until to the backside of the inlet valve. Two small but highly concentrated wall-wetting areas can be spotted in the upside of the inlet port adjacent to the water injector tip. As introduced in Section 2, the injector used in this test is a six-hole injector with a spray cone angle of 34° and a 17° bent axis. It is placed in 10 cm upstream of the inlet valve with a 30° bent angle between the intake port horizontal plane. This installation makes the two upside spray plumes may easily collide onto the topside of the intake port and the rest four downside spray plumes can wet the bottom side area of the intake port around the inlet valves (Fig. 2). By comparing the water film at 1500rpm and 4850rpm, it can be seen that for the same amount water injection, the coverage of the water film area is smaller but the thicker at 1500rpm than that at 4850rpm. At 1500rpm, the maximum water film thickness (red area) can be spotted even when the water injection amount is merely 5mg. Most of the water film coverage is in the green color with only the lightest wall-wetting (blue area) at the edge of the water film. At 4850rpm, the coverage of the water film is large. For the water injection amount of 17mg, almost the entire inner downside of the intake port is covered with the water film. The differences in

water film distribution and formation at 1500rpm and 4850rpm should mainly attribute to the different intake air velocity. For 4850rpm, the intake air jet stream may easily distort the water spray pattern and decrease the momentum when water colliding on the intake port inner surface, which decreases the thickness of water film and disperses the water droplets to the downstream of the intake port. For 1500rpm, the kinetic energy of the intake air is not as strong as that at 4850rpm, resulting in severe wall-wetting. Fig. 12 shows that the water film coverage after the inlet valve closing (left column) only shows moderate shrink comparing with them at the maximum (middle column) at all tested conditions. This indicates a slow evaporation speed of water film. The left column of Figure 12 also shows the in-cylinder water film distribution after the inlet valve is closed. Clearly, at both 1500rpm and 4850rpm, the in-cylinder wall wetting becomes severe as the increase of the PWI amount. At 1500rpm, the water film is mainly scattered around the cylinder wall and the roof. At 4850rpm, the water film area is mainly concentrated at the junction between the cylinder wall and the roof with the only exception for water injection amount of 10mg where wall wetting is light and the distribution of water film is sporadic.

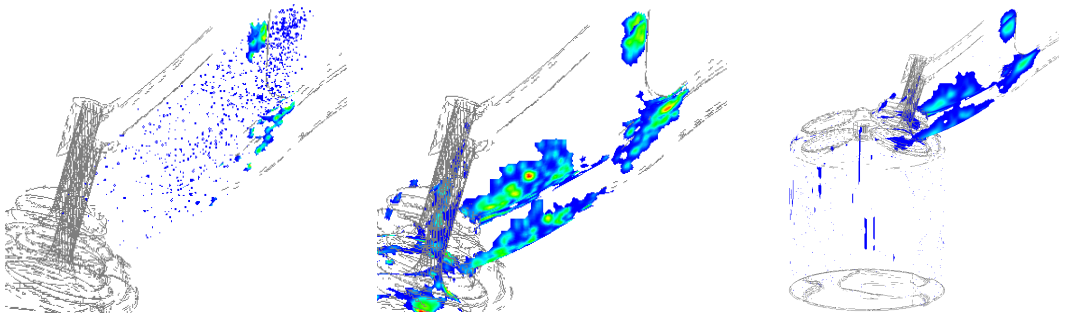

367 °CA 397 °CA 600 °CA

Water injection amount of 10 mg

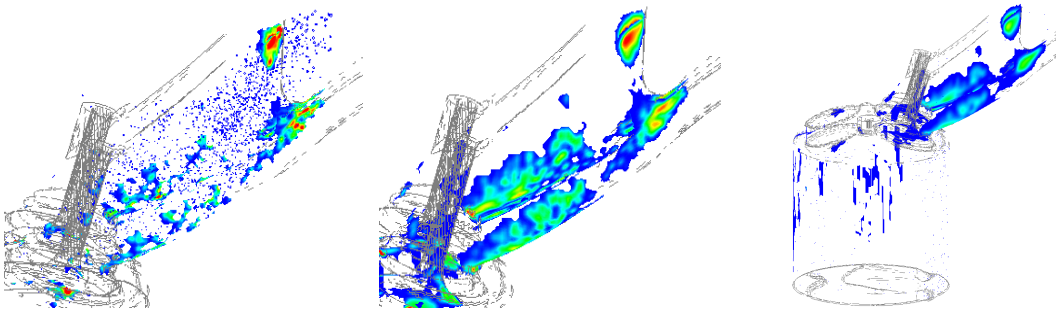

377 °CA 407 °CA 600 °CA

Water injection amount of 17 mg

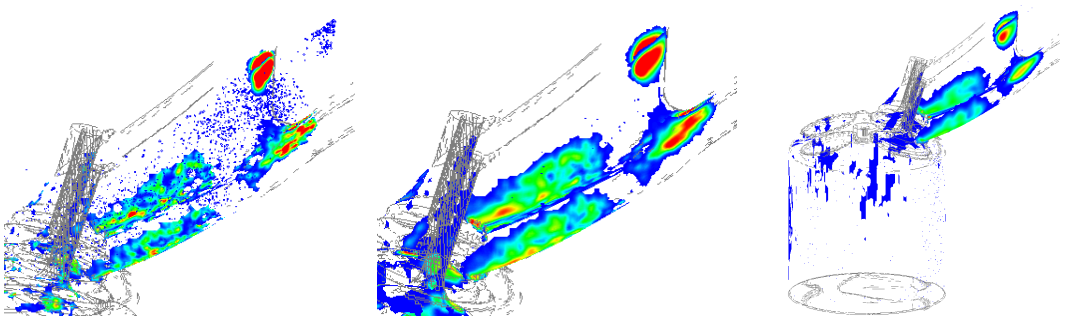

387 °CA 417 °CA 600 °CA

Water injection amount of 25 mg

454 (a)

455

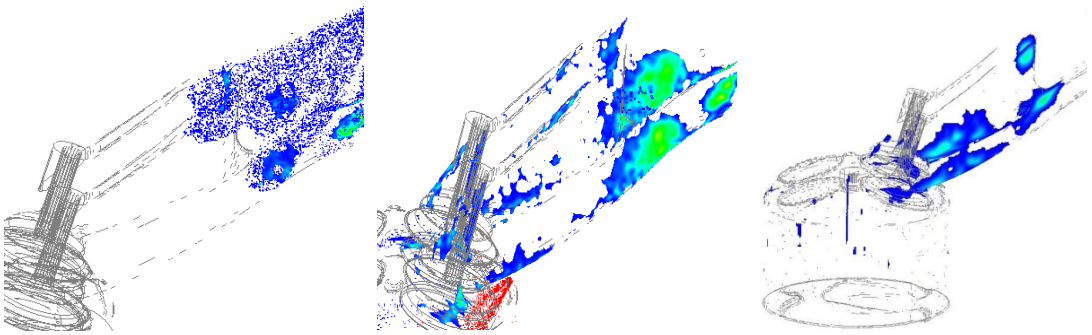

390 °CA 440 °CA 650 °CA

Water injection amount of 10 mg

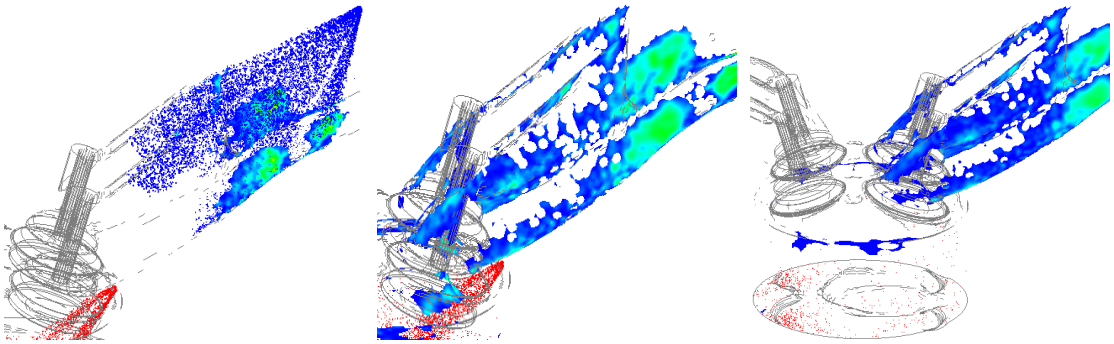

410 °CA 460 °CA 650 °CA

Water injection amount of 17 mg

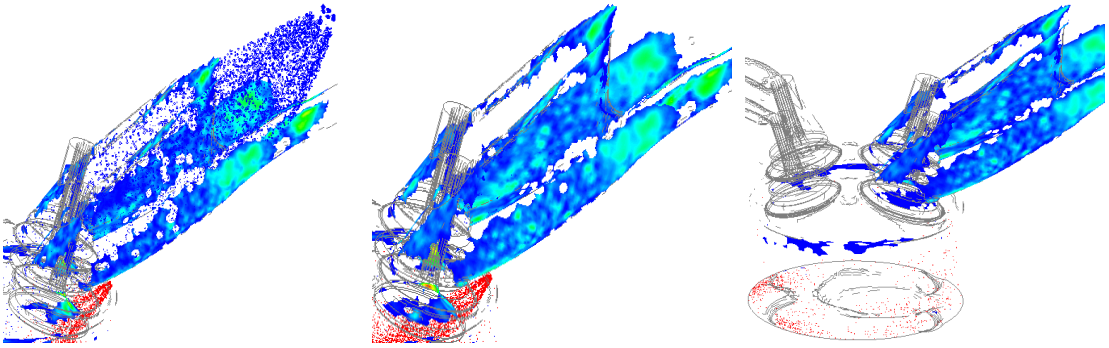

450 °CA 550 °CA 650 °CA

Water injection amount of 25 mg

(b)

Fig. 12. Intake port water wall film distribution at different water injection amount and speed (a) 1500rpm WOT; (b) 4850rpm WOT

Figs. 12 and 13 are illustrated to quantitative analyse the water evaporation process. The variation of water vapor from different sources is demonstrated in Fig. 13. At both 1500rpm and 4850rpm, almost 80% of injected water (blue line) is first impinged on the intake port wall, regardless of the injection amount (orange line). Then the water film gradually vaporizes by absorbing heat from the intake port and the water vapor raises progressively (grey line). As the temperature of fresh charge after the intercooler is far from the boiling point of the water (100° C), the quantity of evaporated water is little (yellow line). However, a minimal increase can be observed before the inlet valve closing (596.5° CA @1500rpm; 628.5° CA @4850rpm). This should be attributed to the backflow of the fresh charge which absorbs the heat in the cylinder and goes back to the intake port, increasing the charge temperate and facilitating the water droplets evaporation. It should be noted that the mesh of the intake port part is discarded after the inlet valve is closed for saving computation resources. Thus, the water vapor evaporated from film and air is grounded to zero after the inlet valve is closed. By comparing 1500rpm and 4850rpm, the quantity of water colliding on the wall accumulates almost perpendicularly at 1500rpm. At 4850rpm, this trend is interfered, making the accumulative curves not smooth with zigzag in the middle. This phenomenon is obvious at low water injection amount (7mg). The relatively high intake air velocity and thermal load at 4850rpm should be the reason for this result. It also can be seen that the quantity of water evaporated from water film in 1500rpnm is greater than that at 4850rpm due to

reduced time for evaporation, albeit the high engine speed raises the intake airflow. Another obvious difference is that not all water vapor enetres the cylinder (dark blue line) at 1500rpm, while almost all the water vapor is sucked into the cylinder at 4850rpm. The relatively high intake air velocity and corresponding VVT control strategy should be the factors that contribute to the above results.

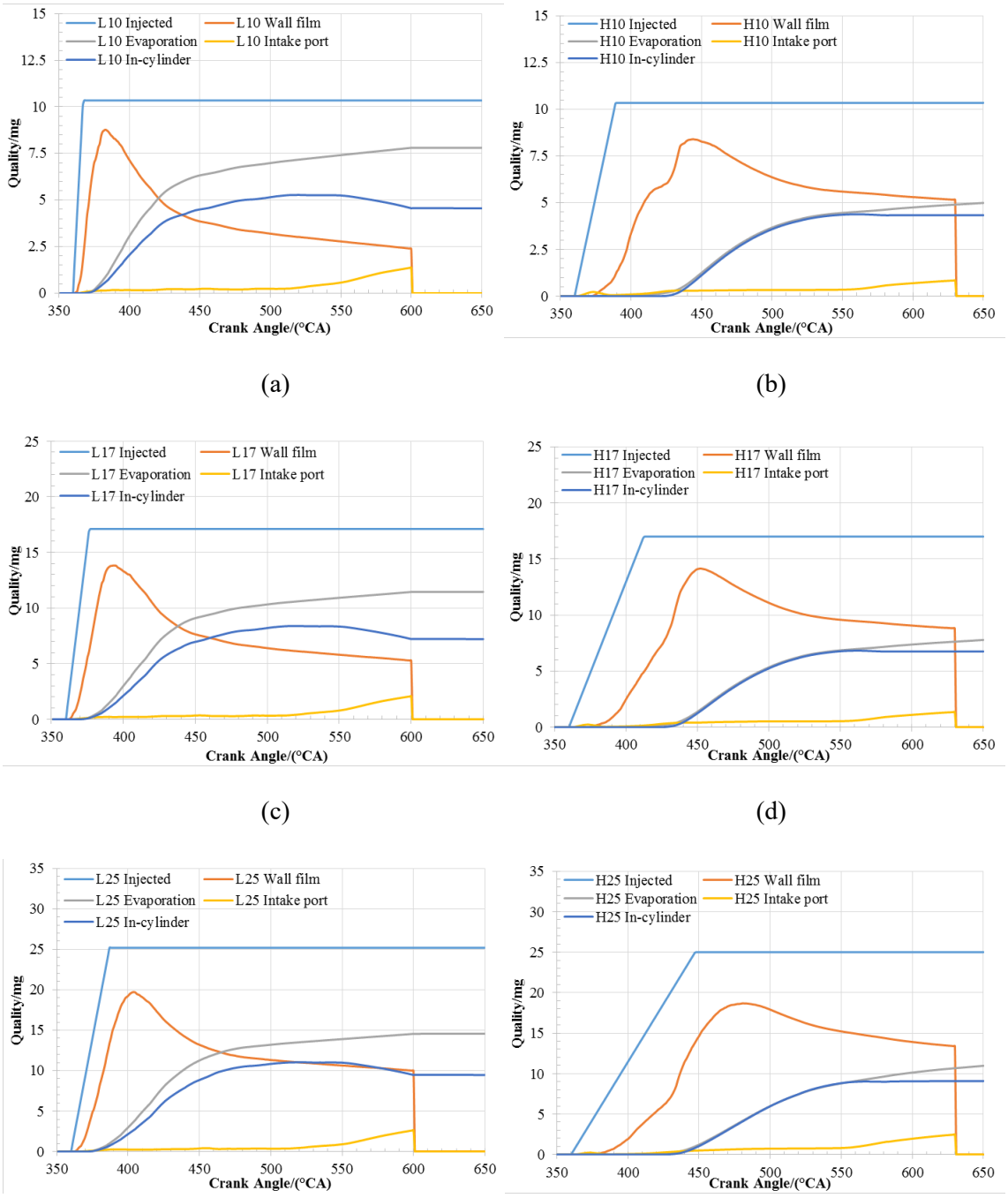

Fig. 13. Variations of water vapor from different sources with crank angle

(a) Water injection amount of 10mg @1500rpm; (b) Water injection amount of 10mg @4850rpm

488 (c) Water injection amount of 17mg @1500rpm; (d) Water injection amount of 17mg @4850rpm
489 (e) Water injection amount of 25mg @1500rpm; (f) Water injection amount of 25mg @4850rpm
490

491 The percentages of water by the time of IVC is shown in Fig. 14. As it is clearly seen that the percentage
492 of wall film at 4850rpm is larger than that at 1500rpm at all the three water injection amounts. The percentage
493 of water vapor evaporated from the wall film at 4850rpm, however, is less than that at 1500rpm. This makes
494 the total share of effective water entering the cylinder are almost the same. At 1500rpm, the percentage of
495 water lost in the scavenging process is larger than that at 4850rpm and the share of water droplets goes into
496 the cylinder is also high at 1500rpm. The relatively large valve overlap angle (Table 1) is the main contributor.
497 Further, the share of water vapor trapped in the intake port by the time of intake valve closing is greater at
498 1500rpm than that at 4850rpm. The 4850rpm condition is more favorable for water evaporation in the air than
499 1500rpm condition. Generally, the total share of water vapor sucked into the cylinder is relatively low, around
500 25% at the tested conditions. This indicates that improving water evaporation rate is imperative for PWI
501 strategy. In this test, a relatively high water injection pressure of 5 MPa is iused with the original purpose of
502 improving primary breakup as suggested by Hoppe et al. [27]. However, this strategy does not show much
503 effect. The real amount of water evaporated in the air is low. Combining the results shown in Fig. 12, the water
504 injector installed in the upstream of intake port just after the intercooler and with a relatively high injection
505 pressure may be an optimal option for giving enough time for water vapor formation. This strategy will be
506 used in future investigation.

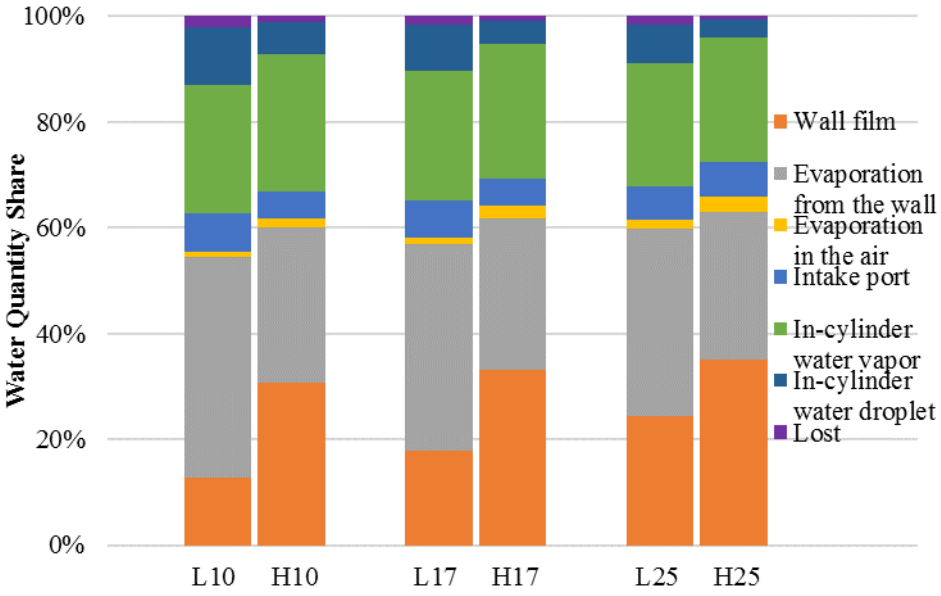

507

508 **Fig. 14.** Share of water at IVC (lenged text can be improved)

509 ***5.3 Influence of PWI on the in-cylinder mixture formation process***

510 In PWI strategy, the engine inhales a large quantity of water vapor and a certain amount of water droplets.
511 The wall film is also formed in part of the cylinder due to the collsion of those water droplets on the wall. All
512 these factors may influence the mixture formation process. Fig. 15 shows the distribution of in-cylinder
513 gasoline wall film (100° after gasoline injection which corresponde to 45° and 62° BTDC for 1500rpm and
514 4850rpm, respectively) and the equivalence ratio by the time of spark discharge. As shown in Fig. 15, 1500rpm
515 results in severer gasoline wall wetting than 4850rpm, and the gasoline wall film area increases with the rise
516 of the water injection amount. For 4850rpm, the in-cylinder temperature (thermal load), turbulence level, and
517 intake air speed are all greater than that at 1500rpm, which can expedite the gasoline fuel droplets evaporation
518 and interaction with the fresh charge. The in-cylinder water film and the water droplets evaporation may
519 substantially bring down local temperature due to the great latent heat of evaporation of water, resulting in
520 lower gasoline fuel evaporation. Thus, more gasoline wall wetting is expected as the raise of water injection
521 amount. At 1500rpm, it also can be seen that the gasoline wall film is mainly concentrated at low half of the
522 cylinder wall opposite the intake valve and gasoline injector. This area is in accordance with the water wall
523 film area as illustrated in Fig. 12. At 4850rpm, an obvious gasoline wall wetting area can be spotted at the
524 junction between the cylinder wall and the piston just beneath the exhaust valve. At the water injection amount

525 of 25mg, gasoline wall film is formed at the edge of the cylinder roof which is also the area where water film

526 is found.

527

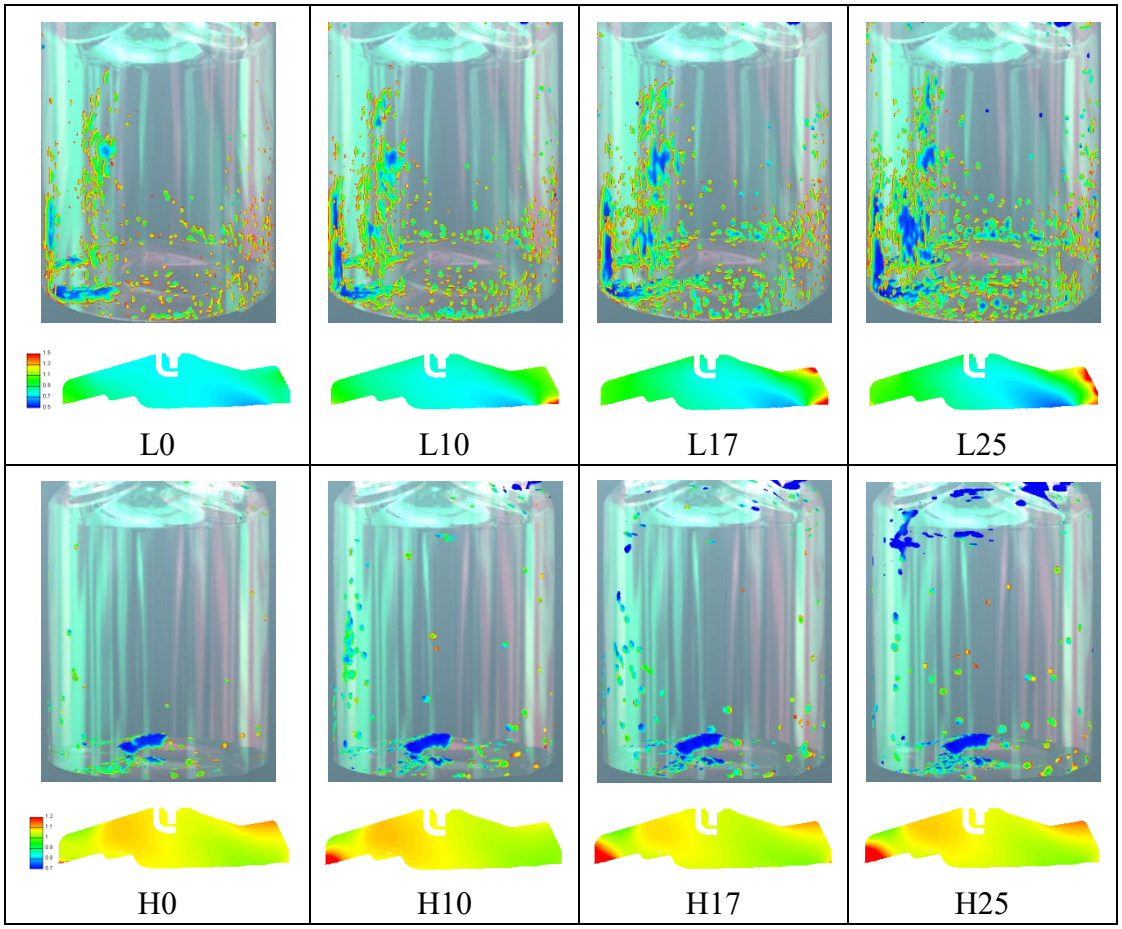

528 **Fig. 15.** In-cylinder water distribution and equivalent ratio

529

530 The general equivalent ratio has not been interfered as the increase of the water injection amount. However,

531 a gasoline-rich area is formed in the right side (intake side) for 1500rpm and left side (exhaust side) for

532 4850rpm with the raise of water injection amount. This may be because the water evaporation reduces the local

533 temperature and gasoline evaporation speed, thus the gasoline fuel cannot be vaporized rapidly and moved

534 with in-cylinder air motion to be distributed uniformly.

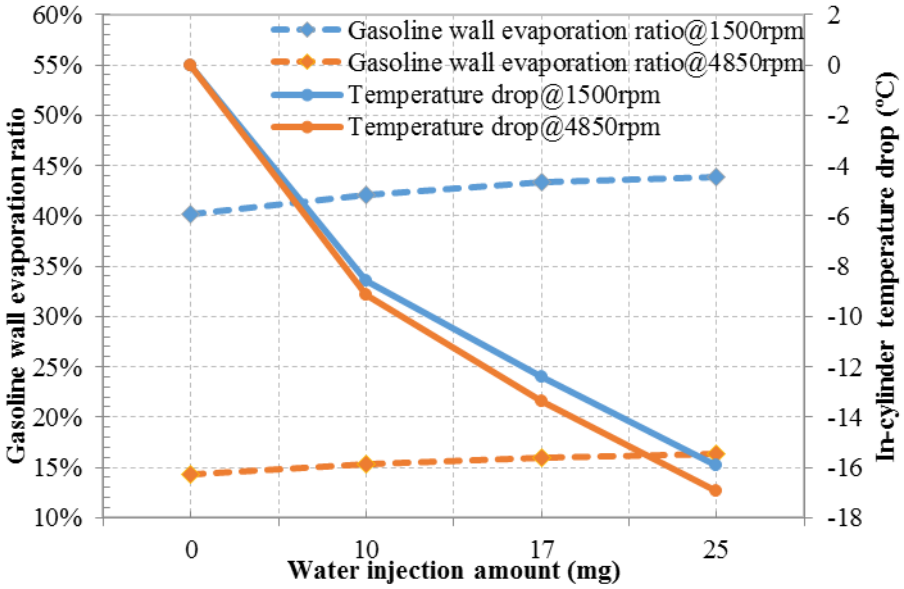

Fig. 16. Variation of temperature drop and wall evaporation ratio with water injection amount

Fig. 16 quantifies the gasoline wall evaporation ratio and the temperature drop due to in-cylinder water film and droplets evaporation. In line with the results shown in Fig. 14, the gasoline vaporized from the wall at 1500rpm is (~40%) greater than that at 4580rpm (~15%). With the increase of water injection amount, the gasoline evaporated from wall raises at both tested speeds. PWI can continuously reduce the in-cylinder temperature after the intake valve is closed due to the evaporation of in-cylinder water film and droplets. At water injection amount of 25mg, a maximum of 16K and 17K temperature drops are achieved for 1500rpm and 4850rpm, respectively. This result corroborates previous studies claiming that the installation of water injector close to the inlet valve is a "quasi-direct" water injection. It is because the port-injected water needs a relatively long time for complete evaporation, and an injector placed close to the inlet valve can inject more water droplets into the cylinder rather than water vapor, which leads to similar effect as that of in-cylinder water injection.

6. Conclusion

In this study, the effect of PWI on engine performance was experimentally and numerically studied at WOT with engine speeds of 1500rpm and 4850rpm, which represent high knocking propensity and the full

553 load with fuel enrichment conditions, respectively. The port water injector was placed as close to the intake
554 valve as possible (10cm upstream the intake valve) to realize a “quasi-direct” effect. Three water injection
555 amounts of 10mg, 17mg and 25mg were tested for each engine speed. Firstly, engine experiments were
556 performed to demonstrate the influence of PWI on knock mitigation, power enhancement, combustion and
557 emissions. Then, numerical simulation was undertaken with a focus on the water spray evolution process,
558 including water droplet evaporation and wall wetting on the intake port and cylinder. The following main
559 conclusions can be drawn:

560 1. PWI is effective in both mitigating engine knock and removal of fuel enrichment at full load conditions. At
561 full load condition (4850rpm WOT), the thermal efficiency increment reaches 6% when the water injection
562 amount is 25mg, thanks to the synthetical effects of knock suppression and fuel enrichment avoidance. At
563 1500rpm WOT condition, where only knock suppression is needed, the thermal efficiency improvement is
564 3.8%.

565 2. PWI provides substantial knock mitigation ability. With the increase of water injection amount from 0 to
566 25mg, the spark timing gradually advances at both tested speeds, CA50 moves forward and major
567 combustion duration (CA10-90) reduces. ISNO and FSN decrease with the rise of water injection amount
568 and ISHC first reduces first then stays stable.

569 3. About 80% of injected water collides on the intake port surface, and the portion of water droplets evaporated
570 in the air is little. By the time of IVC, the water vapor evaporated from water film at 4850rpm is less than
571 that at 1500rpm, which indicates that the time period is important than other factors affecting water wall
572 film vaporization.

573 4. PWI also results in cylinder wall wetting. Higher speed and load may alleviate the in-cylinder wall film due
574 to higher air motion and temperature. The cyinlder water wall wetting negatively affect the cylinder gasoline
575 wall film formation and evaporation. Although the in-cylinder water film can lead to the fuel-rich zone at
576 the corner of the cylinder, the general impact on the in-cylinder equivalent ratio is limited.

References

[1] Huang Y, Ng ECY, Zhou JL, Surawski NC, Chan EFC, Hong G. Eco-driving technology for sustainable road transport: A review. Renew Sustain Energy Rev. 2018;93:596-609.

[2] Huang Y, Surawski NC, Organ B, Zhou JL, Tang OHH, Chan EFC. Fuel consumption and emissions performance under real driving: Comparison between hybrid and conventional vehicles. Sci Total Environ. 2019;659:275-82.

[3] Thewes M, Baumgarten H, Scharf J, Birmes G, Balazs A, Lehrheuer B, et al. Water Injection – High Power and High Efficiency Combined2016.

[4] Lanzafame R. Water injection effects in a single-cylinder CFR engine. SAE International Congress and Exposition. Detroit, Michigan: SAE International; 1999. p. 1-10.

[5] Younkins M, Wooldridge MS, Boyer BA. Port Injection of Water into a DI Hydrogen Engine. SAE Technical Paper Series2015.

[6] Aly H. Gadallah EAEaAME, Hafez A. El-Salmawy, Ahmed H. Bawady. Effect of In Cylinder Water Injection Strategies on Performance and Emissions of a Hydrogen Fuelled Direct Injection Engine. 2009.

[7] Pauer T, Frohnmaier M, Walther J, Schenk P, Hettinger A, Kampmann S. Optimization of gasoline engines by water injection. 37th International Vienna Motor Symposium2016.

[8] Battistoni M, Grimaldi CN, Cruccolini V, Discepoli G, De Cesare M. Assessment of port water injection strategies to control knock in a GDI engine through multi-cycle CFD simulations. SAE Technical Paper Series2017.

[9] Vacca A, Bargende M, Chiodi M, Franken T, Netzer C, Gern MS, et al. Analysis of water injection strategies to exploit the thermodynamic effects of water in gasoline engines by means of a 3D-CFD virtual test bench. 14th International Conference on Engines & Vehicles. Capri, Napoli, Italy: SAE International; 2019. p. 1-16.

[10] De Bellis V, Bozza F, Teodosio L, Valentino G. Experimental and Numerical Study of the Water Injection to Improve the Fuel Economy of a Small Size Turbocharged SI Engine. SAE International; 2017. p. 550-61.

[11] Zhuang Y, Qian Y, Hong G. Lean Burn Performance of a Spark Ignition Engine with an Ethanol–Gasoline Dual Injection System. Energy Fuels. 2018;32:2855-68.

[12] Zhuang Y, Sun Y, Huang Y, Teng Q, He B, Chen W, et al. Investigation of water injection benefits on downsized boosted direct injection spark ignition engine. Fuel. 2020;264:116765.

[13] Hoppe F, Thewes M, Seibel J, Balazs A, Scharf J. Evaluation of the Potential of Water Injection for Gasoline Engines. SAE International; 2017.

[14] Huang Y, Hong G, Huang R. Numerical investigation to the dual-fuel spray combustion process in an ethanol direct injection plus gasoline port injection (EDI + GPI) engine. Energy Convers Manage. 2015;92:275-86.

[15] F. Bedford CR, P. Dittrich, A. Raab, F. Wirbeleit. Effects of Direct Water Injection on DI Diesel Engine Combustion. 2000.

[16] Brusca S, Lanzafame R. Evaluation of the Effects of Water Injection in a Single Cylinder CFR Cetane Engine2001.

[17] Axel O. zur Loye, Omowoleoa C. Akinyemi, Russ P. Durrett, Patrick F. Flynn, Gary L. Hunter, Greg A. Moore, et al. Premixed Charge Compression Ignition Engine with Optimal Combustion Control. In: patents G, editor.: Cummins Inc; 2005.

[18] Lawler B, Mamalis S, Joshi S, Lacey J, Guralp O, Najt P, et al. Understanding the effect of operating conditions on thermal stratification and heat release in a homogeneous charge compression ignition engine. Applied Thermal Engineering. 2017;112:392-402.

[19] Zhuang Y, Ma Y, Qian Y, Teng Q, Wang C. Effects of ethanol injection strategies on mixture formation and combustion process in an ethanol direct injection (EDI) plus gasoline port injection (GPI) spark-ignition engine. Fuel. 2020;268:117346.

[20] Falfari S, Bianchi GM, Cazzoli G, Ricci M, Forte C. Water injection applicability to gasoline engines: Thermodynamic analysis. SAE Technical Paper Series2019.

[21] Cordier M, Lecompte M, Malbec L-M, Reveille B, Servant C, Souidi F, et al. Water injection to improve direct injection spark ignition engine efficiency. WCX SAE World Congress Experience. Detroit, Michigan: SAE International; 2019. p. 1-15.

[22] Meng S, Sun S, Xu H, Guo Y, Feng D, Zhao Y, et al. The effects of water addition on the laminar flame speeds of CO/H2/O2/H2O mixtures. International Journal of Hydrogen Energy. 2016;41:10976-85.

[23] Sun S, Meng S, Zhao Y, Xu H, Guo Y, Qin Y. Experimental and theoretical studies of laminar flame speed of CO/H2 in O2/H2O atmosphere. International Journal of Hydrogen Energy. 2016;41:3272-83.

[24] Kosaka H, Nishigaki T, Kamimoto T, Sano T, Matsutani A, Harada S. Simultaneous 2-D Imaging of OH Radicals and Soot in a Diesel Flame by Laser Sheet Techniques. SAE Transactions. 1996;105:1184-95.

[25] Hajime Fujimoto KK, Go Asai, Jiro Senda. OH Radical Generation and Soot Formation_Oxidation in DI

637 Diesel Engine. 1998.
638 [26] Liu F, Consalvi J-L, Fuentes A. Effects of water vapor addition to the air stream on soot formation and
639 flame properties in a laminar coflow ethylene/air diffusion flame. Combustion and Flame.
640 2014;161:1724-34.
641 [27] Hoppe F, Thewes M, Baumgarten H, Dohmen J. Water injection for gasoline engines: Potentials,
642 challenges, and solutions. International Journal of Engine Research. 2016;17:86-96.
643